Supporting information

A 2D bilayer metal-organic framework as fluorescence sensor for highly selective sensing of nitro explosives

Xiao-Li Hu, Fu-Hong Liu, Chao Qin,* Kui-Zhan Shao and Zhong-Min Su*

Institute of Functional Material Chemistry; Faculty of Chemistry, Northeast Normal University, Changchun, 130024, People's Republic of China; E-mail: qinc703@nenu.edu.cn; zmsu@nenu.edu.cn.

S1. Materials and measurements

All chemical materials were purchased from commercial sources and used without further purification. The FT-IR spectra were recorded from KBr pellets in the range 4000–400 cm^{-1} on a Mattson Alpha-Centauri spectrometer. XRPD patterns were recorded on a Siemens D5005 diffractometer with Cu *Kα* (λ = 1.5418 Å) radiation in the range of 3−60° at a rate of 5°/min. The UV-Vis absorption spectra were examined on a Shimadzu UV-2550 spectrophotometer in the wavelength range of 200-800 nm. The C, H, and N elemental analyses were conducted on a Perkin-Elmer 2400CHN elemental analyzer. TG curves were performed on a Perkin–Elmer TG-7 analyzer heated from room temperature to 1000 ºC at a ramp rate of 5 °C/min under nitrogen. The photoluminescence spectra were measured on a Perkin-Elmer FLS-920 Edinburgh Fluorescence Spectrometer.

S2. X-ray crystallography

Single-crystal X-ray diffraction data for MOF **1** were recorded by using a Bruker Apex CCD diffractometer with graphite-monochromated Mo-K*α* radiation (λ = 0.71069 Å) at 293 K. Absorption corrections were applied by using a multi-scan technique. All the structures were solved by Direct Method of SHELXS-97 and refined by full-matrix least-squares techniques using the SHELXL-97 program within WINGX. Non-hydrogen atoms were refined with anisotropic temperature parameters.

The detailed crystallographic data and structure refinement parameters for MOF **1** are summarized in Table S1.

S3. The solvent sensing experiment

The solvent sensing experiment has been performed as follows: finely ground samples of **1a** was immersed in different organic solvents (3 mL), treated by ultrasonication for 30 minutes, and then aged to form stable emulsions before fluorescence was measured.

Table S1 Crystal data and structure refinement for MOF 1

Formula	$C_{62}H_{69}N_7O_{17}Cd_3$ (**1**)
Formula weight	1521.5
Crystal system	triclinic
Space group	*P*-1
a (Å)	13.530(5)
b (Å)	14.255(5)
c (Å)	19.655(5)
α (°)	73.034(5)
β (°)	74.572(5)
γ (°)	62.256(5)
V (Å^3)	3170.9(18)
Z	2
$D_{calcd.}$[gcm^{-3}]	1.548
F(000)	1492
Reflections collected	18392/11131
R(int)	0.0291
Goodness-of-fit on F^2	1.019
R_1[a] [$I>2\sigma(I)$]	0.0534
wR_2[b]	0.1386

[a] $R_1 = \sum||F_o| - |F_c||/\sum|F_o|$, [b] $wR_2 = |\sum w(|F_o|^2 - |F_c|^2)^2/\sum|w(F_o^2)^2|^{1/2}$

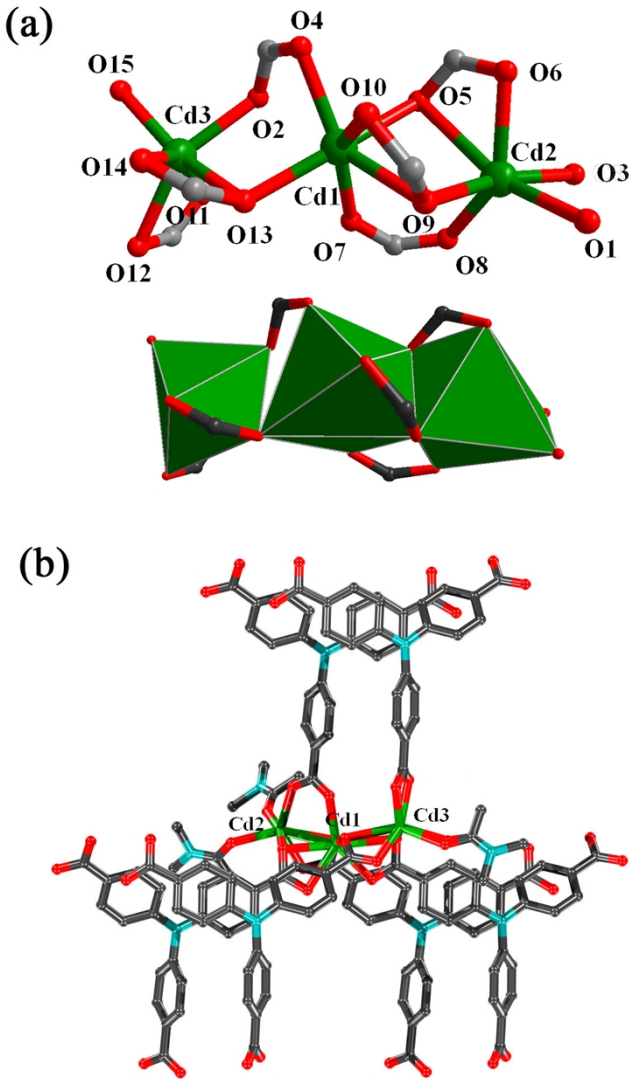

Fig. S1 Coordination environments and the representations of $[Cd_3(CO_2)_6]$ cluster.

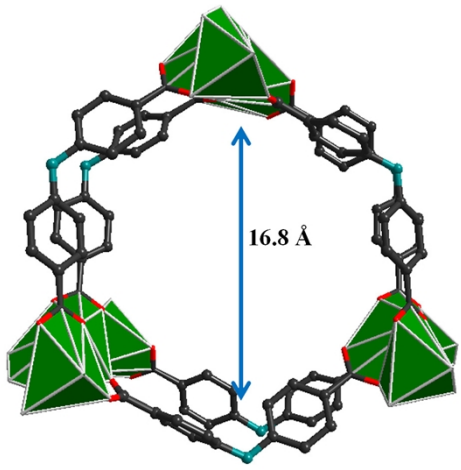

Fig. S2 The view of the 2D bilayer containing hexagonal windows along *c* axis.

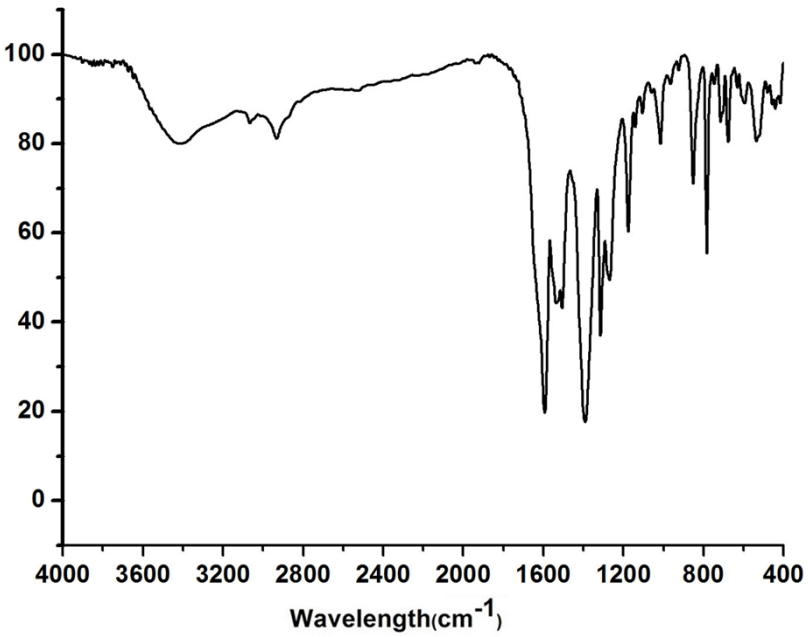

Fig. S3 FT-IR spectra of **1**.

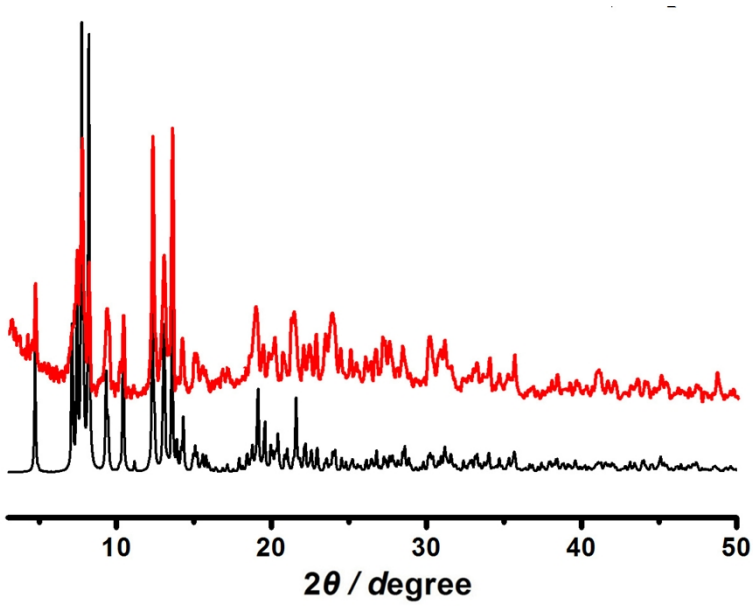

Fig. S4 X-ray powder diffraction patterns of **1**: simulated (black) and as-synthesized (red).

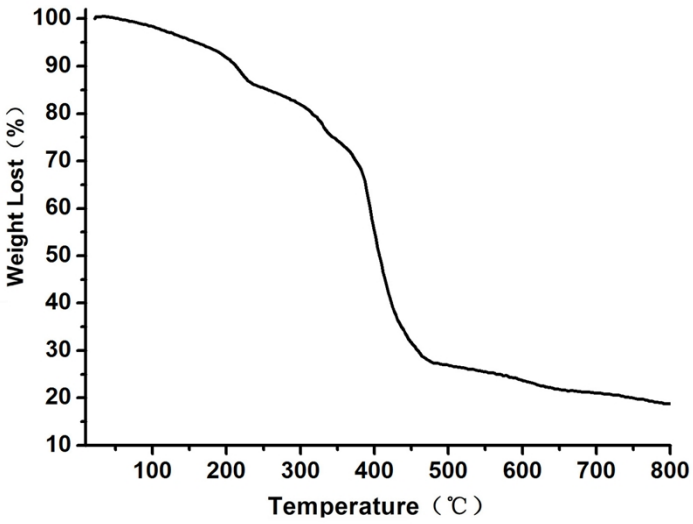

Fig. S5 TG curve of MOF **1**

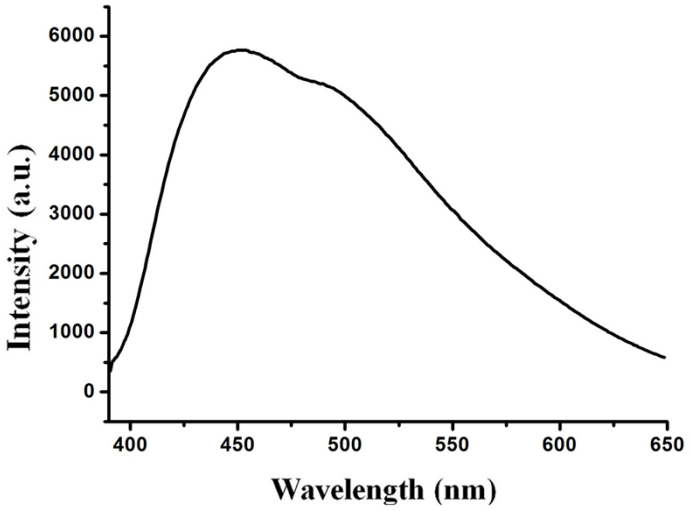

Fig. S6 Emission spectra of the H_3NTB ligand.

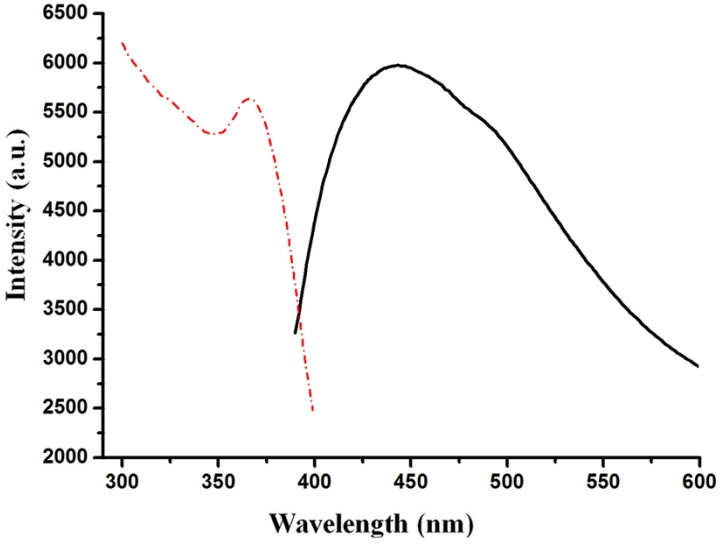

Fig. S7 The excitation (red) and emission (black) spectra of MOF **1**.

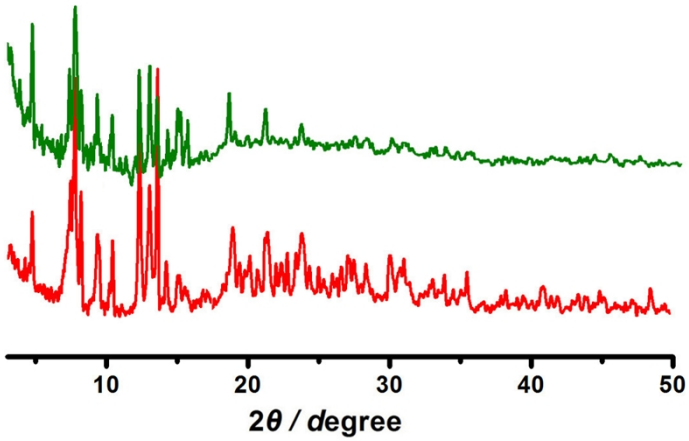

Fig. S8 X-ray powder diffraction patterns of **1**: as-synthesized (red) and after 5 cycles of quenching TNP (green).

Table S2 Selected bond lengths [Å] for MOF **1**

Cd(1)-O(7)#3	2.234(4)	Cd(3)-O(15B)	2.203(17)
Cd(1)-O(4)	2.255(5)	Cd(3)-O(15A)	2.223(12)
Cd(1)-O(13)#4	2.316(5)	Cd(3)-O(14)#4	2.239(5)
Cd(1)-O(5)	2.386(5)	Cd(3)-O(2)	96.2(4)
Cd(1)-O(9)#4	2.402(5)	Cd(3)-O(11)#3	2.430(6)
Cd(1)-O(10)#4	2.436(5)	Cd(3)-O(13)#4	2.531(5)
Cd(1)-Cd(2)	3.4668(11)	O(9)-Cd(2)#2	2.315(5)
Cd(2)-O(8)#3	2.198(5)	O(9)-Cd(1)#2	2.402(5)
Cd(2)-O(3)	2.222(8)	O(10)-Cd(1)#2	2.436(5)
Cd(2)-O(1)	2.259(6)	O(11)-Cd(3)#1	2.430(6)
Cd(2)-O(6)	2.263(5)	O(12)-Cd(3)#1	2.193(5)
Cd(2)-O(9)#4	2.315(5)	O(13)-Cd(1)#2	2.316(5)
Cd(2)-O(5)	2.572(5)	O(13)-Cd(3)#2	2.531(5)
Cd(3)-O(12)#3	2.193(5)	O(14)-Cd(3)#2	2.239(5)

Table S3 Selected bond angles [˚] for **1**

O(7)#3-Cd(1)-O(4)	141.76(19)	O(1)-Cd(2)-O(9)#4	88.1(2)
O(7)#3-Cd(1)-O(13)#4	84.25(18)	O(6)-Cd(2)-O(9)#4	97.7(2)
O(4)-Cd(1)-O(13)#4	97.46(19)	O(8)#3-Cd(2)-O(5)	85.19(18)
O(7)#3-Cd(1)-O(5)	85.55(18)	O(3)-Cd(2)-O(5)	106.9(3)
O(4)-Cd(1)-O(5)	83.87(19)	O(1)-Cd(2)-O(5)	155.0(2)
O(13)#4-Cd(1)-O(5)	164.99(16)	O(6)-Cd(2)-O(5)	53.45(17)
O(7)#3-Cd(1)-O(9)#4	86.68(17)	O(9)#4-Cd(2)-O(5)	84.81(16)
O(4)-Cd(1)-O(9)#4	129.20(18)	O(8)#3-Cd(2)-Cd(1)	74.82(14)
O(13)#4-Cd(1)-O(9)#4	103.14(17)	O(3)-Cd(2)-Cd(1)	147.8(3)
O(5)-Cd(1)-O(9)#4	87.20(17)	O(1)-Cd(2)-Cd(1)	131.34(19)
O(7)#3-Cd(1)-O(10)#4	138.68(17)	O(12)#3-Cd(3)-O(15B)	103.1(5)
O(4)-Cd(1)-O(10)#4	79.54(19)	O(12)#3-Cd(3)-O(15A)	96.3(4)
O(13)#4-Cd(1)-O(10)#4	92.76(18)	O(12)#3-Cd(3)-O(14)#4	150.0(2)
O(5)-Cd(1)-O(10)#4	102.16(19)	O(12)#3-Cd(3)-O(2)	92.3(2)
O(9)#4-Cd(1)-O(10)#4	53.82(17)	O(15B)-Cd(3)-O(2)	100.0(5)
O(7)#3-Cd(1)-Cd(2)	73.13(13)	O(15A)-Cd(3)-O(2)	91.5(3)
O(4)-Cd(1)-Cd(2)	122.47(15)	O(14)#4-Cd(3)-O(2)	109.27(19)
O(13)#4-Cd(1)-Cd(2)	137.68(12)	O(12)#3-Cd(3)-O(11)#3	56.2(2)
O(5)-Cd(1)-Cd(2)	47.89(12)	O(15B)-Cd(3)-O(11)#3	101.3(5)
O(9)#4-Cd(1)-Cd(2)	41.74(12)	O(15A)-Cd(3)-O(11)#3	105.1(4)
O(10)#4-Cd(1)-Cd(2)	82.31(14)	O(14)#4-Cd(3)-O(11)#3	96.43(19)
O(8)#3-Cd(2)-O(3)	93.1(3)	O(2)-Cd(3)-O(11)#3	145.21(19)
O(8)#3-Cd(2)-O(1)	118.7(2)	O(12)#3-Cd(3)-O(13)#4	111.2(2)
O(3)-Cd(2)-O(1)	80.8(3)	O(15B)-Cd(3)-O(13)#4	145.6(5)
O(8)#3-Cd(2)-O(6)	136.9(2)	O(14)#4-Cd(3)-O(13)#4	54.65(16)

O(3)-Cd(2)-O(6)	88.8(3)	O(2)-Cd(3)-O(13)#4	81.18(17)
O(1)-Cd(2)-O(6)	104.1(2)	O(11)#3-Cd(3)-O(13)#4	95.95(18)
O(8)#3-Cd(2)-O(9)#4	88.84(18)	O(15B)-Cd(3)-C(39)#3	104.2(5)
O(3)-Cd(2)-O(9)#4	168.2(3)	O(14)#4-Cd(3)-C(39)#3	123.4(2)
		O(2)-Cd(3)-C(39)#3	119.3(2)